



# Research on the Location of Front-Loading Warehouses Based on the Reverse Logistics of Fresh Agricultural Products

Jiarui XI<sup>1</sup>, Nana GENG<sup>2</sup>

Original Scientific Paper  
Submitted: 26 Apr 2024  
Accepted: 9 Sep 2024

<sup>1</sup> 576953545@qq.com, Nanjing University of Posts and Telecommunications, School of Modern Postal College  
<sup>2</sup> gengnana@njupt.edu.com, Nanjing University of Posts and Telecommunications, School of Modern Postal College



This work is licenced under a Creative Commons Attribution 4.0 International Licence.

Publisher:  
Faculty of Transport and Traffic Sciences,  
University of Zagreb

## ABSTRACT

The proposal to create front-loading warehouses has been suggested as a tactic to enhance the effectiveness and quality of distributing fresh agricultural products in the concluding stage of delivery. Nevertheless, there has been a noted escalation in the rate of loss of these products, which can be ascribed to multiple factors, including inaccuracies in demand forecasting. This incongruity arises from consumers' inability to consume the initially forecasted quantities and unforeseen surges in demand from specific businesses. Consequently, surplus products are left unsold and eventually wasted. This study explores the viability of implementing a reverse logistics model for fresh agricultural products in tandem with the front-loading warehouse. The study presents both traditional and reverse dual models aimed at cost minimisation and introduces novel criteria for the selection of warehouse locations to enhance the efficiency of reverse logistics operations. An advanced hybrid heuristic optimisation algorithm is employed to identify optimal solutions, primarily focusing on minimising product loss rates, reducing logistics expenses and establishing a more equitable supply-demand equilibrium in the area. In the case of Nanjing, it is found that compared with the traditional model, because the network model assumes more functions, the front-loading warehouse in the reverse model has more site selection points in high-demand areas to meet the needs of consumers and is consistent with the distribution of population density and economic activities in Nanjing. At the same time, among the factors affecting the total cost, it is necessary to focus on transportation and fixed costs, while the impact of time and freight damage costs is less.

## KEYWORDS

logistics location; heuristic algorithms; front-loading warehouse; reverse logistics; fresh agricultural products.

## 1. INTRODUCTION

China, with a strong agricultural heritage, has a consistent and significant demand for various agricultural products and by-products each year, necessitating sustained growth. The implementation of front-loading warehouses is a strategic response to current environmental conditions and the need to speed up construction operations in different locations. The current warehouse model limits customers to returning goods that do not meet quality standards or are unwanted due to planning issues. This limitation fails to consider the opportunity to cater to additional customers who may also need these goods. To tackle this challenge, research recommends integrating a reverse logistics model into the front-loading warehouse framework. In contrast to traditional forward logistics, the reverse logistics system in front-loading warehouses allows customers to return excess

or unsuitable goods due to reasons such as inaccurate demand forecasts or changes in plans. Items, whether acquired externally or from customer surplus stock, can be returned to the warehouse for resale or exchange. This process can lead to lower loss rates, increased consumer purchasing incentives and reduced operational expenses for the front-loading warehouse.

To evaluate the feasibility and relevance of the proposed model, this study introduces a new hybrid optimisation algorithm that combines the features of the invasive weed optimisation algorithm and the artificial fish swarm algorithm. This algorithm shows expertise in finding globally optimal solutions rather than getting stuck in local extremes. The system stands out for its quick search capabilities and optimisation efficiency, resulting in the generation of more accurate and effective solutions.

In contrast to prior studies exclusively dealing with front-loading warehouse location issues in forward logistics, this paper integrates the reverse logistics of fresh agricultural products with warehouse location problems and conducts a comprehensive analysis from various cost perspectives. This approach aims to facilitate the retrieval of goods with secondary recovery value for front-loading warehouse purposes, prevent cargo damage, achieve regional supply-demand equilibrium and yield economic benefits. Consequently, compared to traditional network models, the determination of front-loading warehouse locations becomes more intricate as it necessitates consideration of additional influencing factors.

## 2. RELATED RESEARCH

The primary research factors of this article encompass fresh agricultural products, front-loading warehouses and reverse logistics. Presently, there have been research findings on these subjects.

### 2.1 Current status of research on fresh produce

Paulo Almeida [1] et al. proposed and constructed an integrated logistics model for sugarcane harvesting, which was applied to the sugar energy production stage, aiming to improve the operational efficiency in the process of logistics integration. Huimin et al. [2] based on the background of a sudden public health emergency, built an emergency logistics model to ensure the quality of agricultural products during the logistics delivery period and verified the reliability of the model. Jiang et al. [3] developed a comprehensive logistics model for fresh fruit harvesting by considering the issue of fruit ripening. They specified a target function that includes a deviation in fruit ripeness and verified that the model can form a good balance between logistics efficiency and consumer satisfaction. Ulloa et al. [4] believe that special denomination labels have a profound impact on fresh food, and by conducting research, they found that the definition of different labels depends on the potential supply distance of suppliers, and relaxing the regulations on special labels can help reduce carbon dioxide emissions.

### 2.2 The current state of research on the factors that can affect the location of front-loading warehouse

The concept of a front-loading warehouse involves the establishment of a warehouse near a community to address the final stage of distribution for fresh agricultural products, known as the “last kilometre”. This approach is distinct from traditional warehouses located far from the end consumer group and is particularly relevant due to the perishable nature of fresh agricultural products. Fresh e-commerce companies are increasingly adopting pre-warehousing strategies as it allows them to enhance the timeliness of product delivery within more than 3 kilometres from consumers, while also reducing operational costs compared to brick-and-mortar stores. In contrast to conventional warehouses, front-loading warehouses prioritise distribution effectiveness, inventory control, customer flow and related operational aspects. Typically, in cases where a company’s main warehouse is situated at a considerable distance from the urban core, establishing a front-loading warehouse in proximity to end consumers becomes essential to optimise distribution operations and enhance efficiency. The specific research is as follows.

- 1) The discussion of cold chain logistics or time-sensitivity. Chen et al. [5] proposed a time-sensitive vehicle routing problem for cold chain logistics based on warehouse-based distribution, aiming to minimise the cost and discover that the increase of carbon tax can help reduce carbon emissions. Guan et al. [6] have emphasised the growing significance of vehicle distribution factors within contemporary cold chain logistics systems. They have employed an enhanced ant colony algorithm to optimise their formulated planning problem, thereby demonstrating the feasibility of both their experiment and algorithm. Gong et al. [7] explored the impact of time sensitivity and environmental sustainability on competition among

contemporary e-commerce companies from a game theory perspective. Their experimental findings ultimately demonstrated the significance of adhering to promised delivery times.

- 2) Research on considering customer satisfaction and other customer factors. Rahmanifar et al. [8] developed a nonlinear multi-objective model to optimise vehicle routes and warehouse locations to minimise overall costs, while also addressing customer requirements. Li et al. [9] established a multi-objective model that integrated network cost, carbon trading cost and customer satisfaction as primary considerations. Their goal was to improve customer satisfaction while reducing logistics costs. They utilised an enhanced multi-objective algorithm for analysis and confirmed that the proposed method effectively increased customer satisfaction and lowered logistics expenses. This research is significant in academic circles due to its focus on improving customer experience while optimising operational costs. Garai et al. [10] have established a customer-centric and cost-effective closed-loop supply chain model and conducted an analysis using a newly developed semi-autonomous multi-objective optimisation algorithm to obtain the optimal values of the model under uncertain conditions.
- 3) Some research results of the lowest total cost as the main objective. Chen et al. [11] analysed three modes of selling fresh agricultural products at this stage and compared their advantages and disadvantages, to select the most reasonable sales mode for retailers in different environments and conduct a site selection simulation. Jiang et al. [12] proposed a multi-type of drone collaborative delivery model based on the current trend of drone development. By considering factors such as drone energy consumption, payload and warehouse conditions, they minimised the total cost while maximising the efficiency of delivery. They also validated the feasibility of the model using an improved ant colony algorithm. Govindan et al. [13] conducted a study to examine the feasibility of an elastic sustainable reverse logistics network for end-of-life vehicles, with the primary objective of minimising total costs. They demonstrated the practicality of their proposed model using the cross-entropy algorithm.

### 2.3 State of the art of reverse logistics research

Reverse logistics can be defined as the strategic management and coordination of the efficient movement of raw materials, intermediate inventory, finished goods and associated information from the point of consumption back to the origin to recover value or responsibly dispose of these items. This concept diverges from the conventional supply chain model. The following research findings are available.

Alexandre et al. [14] proposed an agent-based simulation tool to predict the performance of a reverse logistics network, and referred to several major factors such as social demographic information and consumption capacity, in order to achieve the maximum return rate and minimise the installation and operation costs. Ermes et al. [15] believed that an important aspect of implementing the omni channel retail strategy is to have an efficient reverse logistics process, and used the general qualitative design of the purpose sampling method to verify their views. Sadra et al. [16] discussed the most effective decision-making strategy in reverse logistics based on consumer feedback, and proposed methods to help manufacturers reduce costs in the context of the increase in the replacement rate of unused electronic equipment by consumers. Bajgani Sahar et al. [17] considering flexibility and cost-effectiveness, finally found that the punishment strategy improved the level of technology acquisition at the cost of reducing the overall profit, while the incentive strategy could maintain the profit colour, but could not significantly improve the level of technology acquisition.

### 2.4 Related research on location

Yi et al. [18] studied the location of intercity railway stations with the goal of obtaining economic profits, and designed a general algebraic modelling system with linear programming for simulation tests, verifying the profit feasibility of the proposed model. Ou et al. [19] have conducted in-depth research on the location of intermodal transport hubs for road-railway multimodal transport, to improve railway transport capacity and promote the development of low-carbon transport. They used data mining technology to build a mathematical model and found that the proposed model can effectively reduce carbon emissions, and verified its practicability. Zhongyi et al. [20] discussed the location problem of a new UAV rescue facility and established a Semblu rod optimisation model to solve the demand uncertainties. The experiment verifies that the proposed model has superior performance in the humanitarian aid logistics system, and measures the risk control in the humanitarian aid logistics system. Jiatong et al. [21] focused on considering the roaming delay cost of users, and established a double-layer optimisation problem with the goal of maximising social welfare, aiming to solve the problem of station location for shared bicycles. They use the genetic algorithm and rolling horizon method to solve the upper and lower-level problems respectively, confirm the performance of the algorithm, and provide ideas for location problem planning. Kitthamkesorn et al. [22] conducted an in-depth discussion on the location problem of park-and-ride facilities and developed a PCW model for solving and analysis. During the study, they found that route overlap and fare structure have a significant

impact on the number of users and the optimal location of the facility. Abdulvahitoğlu et al. [23] sorted out the traffic accidents in a certain region of Turkey, combined with the number of local traffic gendarmes, used mixed integer programming to conduct modelling analysis, and determined the optimal result of the location of the traffic gendarmes in this region.

## 2.5 The shortcomings and deficiencies of current traditional models

Current research on the pre-positioning warehouse logistics model for fresh agricultural products primarily focuses on cold chain logistics, low-carbon logistics and route planning and optimisation. However, existing studies have not yet integrated reverse logistics as a significant factor in the model's site selection considerations. Recent research findings and data reports indicate a rising annual waste rate of fresh agricultural products, leading to challenges in meeting increasing demand. Consequently, exploring the implementation of a reverse logistics model for fresh agricultural products aligns with the evolving logistics landscape in China. Resolving site selection issues related to front-loading warehouses can contribute to addressing supply and demand challenges in this sector.

## 3. MATHEMATICAL MODELLING

The focus in the development of a reverse front-loading warehouse model lies in its reverse segment, requiring comprehensive deliberation.

### 3.1 Model description

In contrast to the conventional front-loading warehouse location model, the reverse location model needs to consider the reverse logistics process from the consumer node to the front-loading warehouse. This implies that in the traditional forward model, the front-loading warehouse serves not only as a supply point for the consumer node but also as a demand point for receiving goods sent from the consumer node. A key distinction from the forward model lies in the fact that the reverse model must account for a range of costs incurred from the consumer to the front-loading warehouse when formulating the total cost objective function, commonly referred to as the reverse cost. The research paper incorporates the reverse logistics model to optimise the utilisation of fresh agricultural products for secondary purposes at the end consumer stage. This approach aims to minimise waste, enhance sustainability and contribute to achieving equilibrium between supply and demand in the agricultural sector.

### 3.2 Constructing abstract network diagrams

The network nodes in the conventional model and the reverse model proposed in this study primarily consist of large-scale distribution centres or hubs, front-loading warehouses and end users. Initially, goods are transported from the distribution centre to the front-loading warehouse before being distributed to consumers via the intermediate warehouse. In the reverse model, an additional step involves consumers delivering goods to the front-loading warehouse. The abstract network diagram construction and local schematic diagram of the front-loading warehouse reverse logistics siting model in this paper are shown in *Figures 1 and 2*.

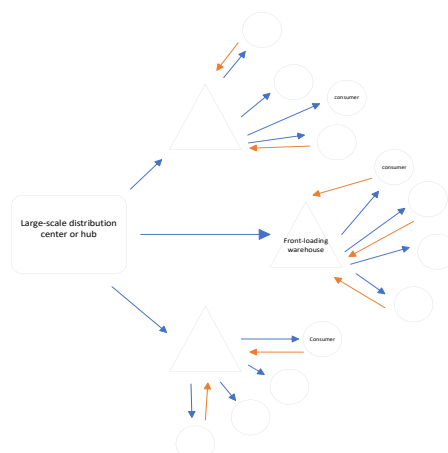


Figure 1 – Abstract network diagram

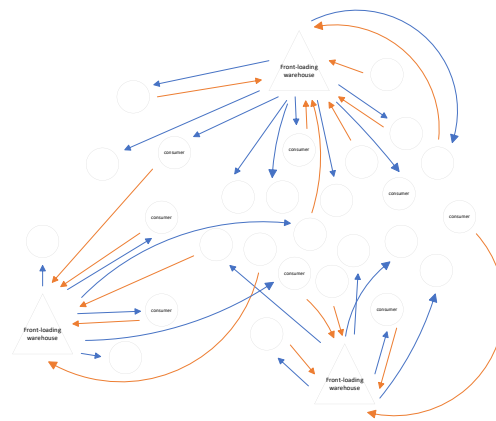


Figure 2 – Partial schematic diagram

Based on the classification of node types, the conventional warehousing location issue can be categorised into three tiers: large-scale distribution centre or hub, front-loading warehouse and consumer. Within this network configuration, there exist two stages: large-scale distribution centre to front-loading warehouse and front-loading warehouse to consumer. The newly introduced reverse front-loading warehouse model encompasses the consumer to front-loading warehouse segment, thus comprising three stages. In contrast to the conventional approach, the reverse model necessitates the amalgamation of the third stage with the initial two stages, thereby requiring more precise and responsive data support for determining the location of the front-loading warehouse.

### 3.3 Model assumptions

(1) Each front-loading warehouse being evaluated has access to goods from the previous node and the consumer node exclusively, with no other sources available. (2) Within the consumer node of the model, consumer goods can be acquired from the preceding node of the front-loading warehouse or through alternative channels. (3) Information regarding distribution distances and times is provided and considered in the analysis. (4) The model does not account for the specific type and performance of distribution vehicles. (5) External factors like weather conditions that may impact distribution are not factored into the model. (6) Contingencies are not included in the model, and factors influencing contingencies are excluded from consideration. (7) Goods are categorised as fresh agricultural products without further subcategorisation. (8) Fixed unit costs, such as freight charges, are assumed and do not vary based on changes in distance or time.

### 3.4 Model cost analysis

The overall expenses associated with the front-loading warehouse reverse logistics siting model encompass six categories, mirroring those of the forward siting model. A distinguishing factor between the reverse and forward location models is the necessity to account for a range of additional costs incurred by consumers in relation to the front-loading warehouse. The following is a description of the decision variables and parameters.

- $N = \{1, 2, 3, \dots, n\}$  the collection of large distribution centres or hubs
- $I = \{1, 2, 3, \dots, i\}$  the collection of supply points
- $J = \{1, 2, 3, \dots, j\}$  the collection of demand points
- $C_n$  the fixed cost of the large distribution centre or hub  $n (n \in N)$
- $C_i$  the fixed cost of the  $i$ th front-loading warehouse ( $i \in I$ )
- $C_j$  the fixed cost of the  $j$ th demand point in the consumer node ( $j \in J$ )
- $a_n$   $\begin{cases} 1, \text{select the large distribution center or hub } n (n \in N) \\ 0, \text{otherwise} \end{cases}$

|                         |  |
|-------------------------|--|
| $a_i$                   | $\begin{cases} 1, \text{select the supply point } i (i \in I) \\ 0, \text{otherwise} \end{cases}$  |
| $a_j$                   | $\begin{cases} 1, \text{select the requirement point } j (j \in J) \\ 0, \text{otherwise} \end{cases}$   |
| $cq$                    | the unit cost of transportation  |
| $q$                     | volume of cargo transport in the corresponding stage   |
| $q_{ni}^k$              | the cargo transportation volume from a large distribution centre or hub $n (n \in N)$ to front-loading warehouse $i (i \in I)$   |
| $q_{ij}^k$              | the cargo transportation volume from the front-loading warehouse $i (i \in I)$ to the consumer $j (j \in J)$   |
| $d$                     | transport distance of goods in the corresponding stage   |
| $d_n^k$                 | the transportation distance from large distribution centre $n (n \in N)$ to front-loading warehouse $i (i \in I)$  |
| $d_{ij}^k$              | the transportation distance from the front-loading warehouse $i (i \in I)$ to consumer $j (j \in J)$   |
| $q_{ji}^k$              | the cargo transportation volume from consumer $j (j \in J)$ to front-loading warehouse $i (i \in I)$   |
| $d_{ji}^k$              | the transportation distance from consumer $j (j \in J)$ to front bin $i (i \in I)$   |
| $k$                     | $\begin{cases} 1, \text{select the point} \\ 0, \text{otherwise} \end{cases}$ , means whether the desired decision point is selected in the decision variable, such as $n, i, j$ , etc ( $n \in N, i \in I, j \in J$ ) |
| $c_t$                   | the cost per unit of time  |
| $t$                     | the corresponding stage of cargo transport time  |
| $t_{ni}^k$              | the delivery time from a large distribution centre or hub $n (n \in N)$ to a front-loading warehouse $i (i \in I)$   |
| $t_{ij}^k$              | the delivery time from a front-loading warehouse $i (i \in I)$ to consumer $j (j \in J)$   |
| $t_2$                   | the remaining time (loading and unloading time, etc.) in the stage except for transportation   |
| $t_{ji}^k$              | the transportation time from consumer $j (j \in J)$ to front-loading warehouse $i (i \in I)$   |
| $f$                     | the penalty coefficient for cargo loss   |
| $s_1$                   | the rates of cargo loss during transportation  |
| $s_2$                   | the rates of cargo loss during non-transportation  |
| $C_s$                   | the unit cost of damage to goods   |
| $q (s_1/s_2)$           | the freshness of the goods delivered to the destination within the distance  |
| $\mu (s_1/s_2)$         | dedicate to maintaining freshness  |
| $\varepsilon$           | the natural decay rate of goods  |
| $f_2$                   | the value of the time penalty coefficient  |
| $t_i/t_j/t_{ji}$        | the actual delivery time   |
| $t_{ik}/t_{jk}/t_{jik}$ | the best delivery time of the plan   |
| $C_{m1}$                | the cost of satisfaction with the quantity of goods  |
| $C_{m2}$                | the cost of satisfaction with the freshness of the goods   |
| $C_{m3}$                | the cost of satisfaction with convenience  |
| $o$                     | customer convenience rate  |
| $m$                     | customer satisfaction coefficient  |
| $\alpha/\beta/\gamma$   | weighted rates   |
| $G$                     | the pricing appropriateness rate   |
| $C_{m4}$                | the cost of satisfaction with the recovery price   |

|           |  |
|-----------|--|
| Y         | the budget's upper limit   |
| $s_d$     | the cost saved by transportation   |
| $\Omega$  | the price estimate or recovery intention of the recovered goods                                      |
| p         | the normal retail price  |
| $\varphi$ | dynamic factors  |
| u         | the sensitivity coefficient of freshness   |
| $C_p$     | the cost per unit of carbon emissions  |
| e         | the emission factor for CO <sub>2</sub>  |
| $V_h$     | the capacity of the front-loading warehouse  |
| $U_n$     | the total capacity of large distribution centres or hubs n ( $n \in N$ )                             |
| w1        | the unit energy consumption of transport vehicles from N ( $N \in R$ ) to I ( $I \in R$ )            |
| w2        | the unit energy consumption of transport vehicles from I ( $I \in R$ ) to J ( $J \in R$ )            |
| w3        | the unit operation and construction energy consumption of front-loading warehouses based on capacity |

1) Fixed cost. Fixed cost is the cost that is not related to a series of operations, such as the transportation of goods, and does not change throughout the network structure. Fixed costs in this paper include the construction costs of large distribution centres or hubs, the construction costs of front-loading warehouses and the network costs of consumer nodes. The total fixed cost C1 is Equation 1:

$$C1 = \sum_{n=1}^N c_n a_n + \sum_{i=1}^I c_i a_i + \sum_{j=1}^J c_j a_j \tag{1}$$

of which,  $a_n = \begin{cases} 1, & \text{select the large distribution center or hub} \\ 0, & \text{otherwise} \end{cases}$

$a_i = \begin{cases} 1, & \text{select the supply point} \\ 0, & \text{otherwise} \end{cases}$

$a_j = \begin{cases} 1, & \text{select the requirement point} \\ 0, & \text{otherwise} \end{cases}$

2) Transportation cost. Transportation cost is the cost of transportation between two points, which is mainly related to transportation distance and transportation volume. Then the total transportation cost C2 is Equation 2:

$$C2 = \sum_{n=1}^N \sum_{i=1}^I c_q q_{ni}^k d_{ni}^k a_n a_i + \sum_{i=1}^I \sum_{j=1}^J c_q q_{ij}^k d_{ij}^k a_i a_j + \sum_{i=1}^I \sum_{j=1}^J c_q q_{ji}^k d_{ji}^k a_i a_j \tag{2}$$

where k denotes the cumulative coefficient,  $k = \begin{cases} 1, & \text{select the point} \\ 0, & \text{otherwise} \end{cases}$

3) Cost of time. Time cost refers to the cost calculated from the amount of time consumed in the whole logistics operation process. In the model of this paper, it specifically includes transportation time and cargo loading and unloading time. Then the total time cost C3 is Equation 3.

$$C3 = \sum_{n=1}^N \sum_{i=1}^I t_{ni}^k c_t a_n a_i + t_2 c_t + \sum_{i=1}^I \sum_{j=1}^J (t_{ij}^k + t_{ji}^k) c_t a_i a_j \tag{3}$$

4) Penalty cost. In this part, the main consideration of the transportation process of cargo loss rate and non-transportation process of cargo loss rate (loading and unloading handling, etc.), as well as distribution to the place of the time beyond the prescribed time and the overflow time penalty cost, which the cargo loss rate indicators with the transportation of goods, and the overflow time with the upper limit of the prescribed time. The portion of the penalty cost of damage to goods in the penalty cost is Equation 4.

$$\sum_{n=1}^N \sum_{i=1}^I \sum_{j=1}^J (q_{ni}^k + q_{ij}^k) s1 c_s a_n a_i a_j f + \sum_{n=1}^N \sum_{i=1}^I \sum_{j=1}^J (q_{ni}^k + q_{ij}^k) s2 c_s a_n a_i a_j \tag{4}$$

Among them, Liu et al. [24] think that the freshness of goods is a function relative to the transportation distance and have constructed a freshness formula suitable for cold chain logistics and fresh agricultural products in this paper. The dynamic differential equation of freshness is Equation 5 as follows.

$$q'(s) = \frac{dq}{ds1 / ds2} = \mu(s1 / s2) - \varepsilon \tag{5}$$

For the time-penalty cost component, the design of the time window with respect to the time-penalty coefficient f2 is shown in Figures 3 and 4 as follows.

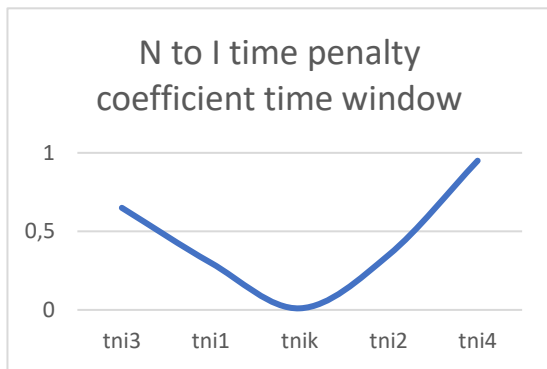


Figure 3 – N to I time window



Figure 4 – I to J time window

As shown in the figure, [tni1, tni2] and [tij1, tij2] represent the time window of expected delivery, and [tni3, tni4] and [tij3, tij4] represent the acceptable time window of delivery. Therefore, time penalty cost C4(t)<sub>1</sub> for Equation 6:

$$C4(t)_1 = \begin{cases} \inf, & t_i < tni3, t_j < tij3 \\ \frac{|t_i / t_j - tnik / tijk|}{(t_i / t_j) * f2^{|t_i/t_j - tnik/tijk|}}, & tni3 / tij3 \leq t_i / t_j < tni1 / tij1 \\ \frac{|t_i / t_j - tnik / tijk|}{(1-f2)^{|t_i/t_j - tnik/tijk|}}, & tni1 / tij1 \leq t_i / t_j \leq tni2 / tij2 \\ \frac{|t_i / t_j - tnik / tijk|}{|t_i / t_j - tnik / tijk| * f2^{|t_i/t_j - tnik/tijk|}}, & tni2 / tij2 < t_i / t_j \leq tni4 / tij4 \\ \inf, & t_i > tni4, t_j > tij4 \end{cases} \tag{6}$$

The portion of the cost link associated with cargo damage increases the cost of cargo damage in the reverse segment, and the rest of the cost parameters remain unchanged so that the penalty cost of cargo damage Equation 7 is:

$$\sum_{n=1}^N \sum_{i=1}^I \sum_{j=1}^J (q_{ni}^k + q_{ij}^k + q_{ji}^k) s1c_s a_n a_i f + \sum_{n=1}^N \sum_{i=1}^I \sum_{j=1}^J (q_{ni}^k + q_{ij}^k + q_{ji}^k) s2c_s a_n a_i a_j f \tag{7}$$

where, to fit the actual situation, dynamic factors are added to the dynamic differential equation of freshness based on the reverse segment φ, to distinguish the freshness trend of fresh agricultural products in the positive model. Then the dynamic equation of freshness is Equation 8 as follows.

$$q_\phi'(s) = \frac{dq^\phi}{ds1 / ds2} = \phi[\mu(s1 / s2) - \varepsilon]^{-\phi} \tag{8}$$



For the time penalty cost component, the additional design of the time window based on the inverse segment with respect to the time penalty coefficient  $f_2$  is shown in Figure 5.

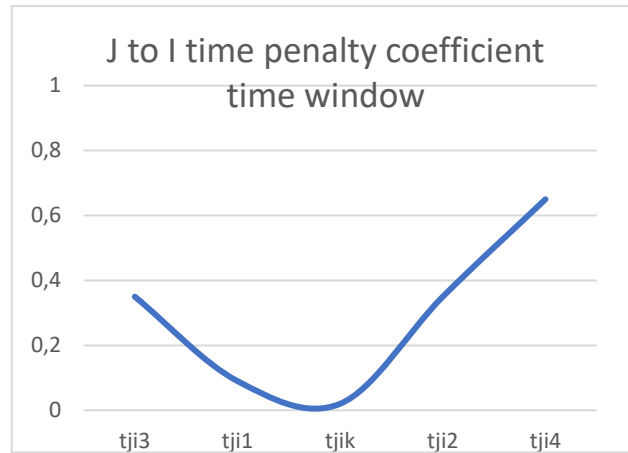


Figure 5 – J to I time penalty factor time window

As shown in the figure above,  $[t_{ji1}, t_{ji2}]$  refers to the expected delivery time window, and  $[t_{ji3}, t_{ji4}]$  refers to the acceptable delivery time window. Time penalty cost  $C4(t)_2$  for Equation 9:

$$C4(t)_2 = \begin{cases} \text{inf}, & t_{ji} < t_{ji3} \\ \frac{|t_{ji} - t_{jik}|^{f_2}}{t_{ji} * f_2^{|t_{ji} - t_{jik}|}}, & t_{ji3} \leq t_{ji} < t_{ji1} \\ \frac{|t_{ji} - t_{jik}|}{(1-f_2)^{[t_{ji}/t_{ji} - t_{jik}/t_{jik}]} * f_2}, & t_{ji1} \leq t_{ji} \leq t_{ji2} \\ \frac{|t_{ji} - t_{jik}|}{|t_{ji} - t_{jik}|^{(1+f_2)} * f_2^{|t_{ji} - t_{jik}|}}, & t_{ji2} < t_{ji} \leq t_{ji4} \\ \text{inf}, & t_{ji} > t_{ji4} \end{cases} \tag{9}$$

where inf represents an infinite positive number. To sum up, the total penalty cost C4 is Equation 10.

$$C4 = \sum_{n=1}^N \sum_{i=1}^I \sum_{j=1}^J (q_{ni}^k + q_{ij}^k + q_{ji}^k) s1 c_s a_n a_i f + \sum_{n=1}^N \sum_{i=1}^I \sum_{j=1}^J (q_{ni}^k + q_{ij}^k + q_{ji}^k) s2 c_s a_n a_i a_j f + C4(t)_1 + C4(t)_2 \tag{10}$$

5) Customer satisfaction cost. Customer satisfaction cost is a cost that changes as customer satisfaction changes. The total customer satisfaction cost C5 is Equation 11.

$$C5 = (\sum_{i=1}^I \sum_{j=1}^J q_{ij}^k a_i a_j c_{m1} + \sum_{i=1}^I \sum_{j=1}^J q_{ij}^k a_i a_j q(s1/s2) c_{m2} + oc_{m3}) m \tag{11}$$

The dynamic calculation formula of customer satisfaction coefficient m is Equation 12 as follows.

$$m = [ \frac{1}{(\alpha * q(s1/s2) + \beta * o + \gamma * G)^{-k}} - (1 - k) ] * 100\% \tag{12}$$

Considering the cost of customer satisfaction in the reverse location model, the cost of satisfaction with the recovery price function is Equation 13.

$$G_{c_{m4}} * m \tag{13}$$

In addition, the upper limit of the budget constraint is added in the reverse section to ensure the economic benefits of the recovery process, building the budget constraint as Equation 14.

$$\int_0^{d_{ji}} 0.5\lambda\mu^2(s1 / s2)d(s) \leq Y \tag{14}$$

In addition, the impact of customer utility needs to be considered when calculating the cost of the reverse segment. Generally, the higher the proportion of customer utility, the higher the economic benefits and the lower the relative cost. In the reverse logistics process of fresh agricultural products, customers place orders through the internet or communication, which can reduce their spending on transportation, which is favourable to other satisfaction cost factors. Therefore, the utility function formula of the unit customer is Equation 15.

$$Z(s) = \Omega + \nu q(s1 / s2) + s_d - p \tag{15}$$

To sum up, the total customer satisfaction cost C5 is Equation 16:

$$C5 = [\sum_{i=1}^I \sum_{j=1}^J (q_{ij}^k + q_{ji}^k) a_i a_j c_{m1} + \sum_{i=1}^I \sum_{j=1}^J (q_{ij}^k + q_{ji}^k) a_i a_j q(s1 / s2) c_{m2} + oc_{m3} + G_{c_{m4}}](1 - m) - Z(s)q_{ji}^k \tag{16}$$

6) Cost of carbon emissions. Carbon emission cost is the cost of carbon dioxide emissions resulting from vehicle transportation, site construction and capacity (this model only focuses on the construction or capacity of the front-loading warehouse) within the entire logistics operation. Therefore, the total carbon emission cost C6 is Equation 17.

$$C6 = c_p e [w1 \sum_{n=1}^N \sum_{i=1}^I d_{ni}^k a_n a_i + w2 \sum_{i=1}^I \sum_{j=1}^J (d_{ij}^k + d_{ji}^k) a_i a_j + w3 \sum_{h=1}^H V_h] \tag{17}$$

### 3.5 Modelling

In summary, the model of front-loading warehouse reverse logistics site selection is constructed in Equations 18-32 as follows.

$$minC = C1 + C2 + C3 + C4 + C5 + C6 \tag{18}$$

$$\sum_{i=1}^I a_i \leq H \tag{19}$$

$$\sum_{n=1}^N \sum_{i=1}^I d_{ni}^k, \sum_{i=1}^I \sum_{j=1}^J d_{ij}^k > 0 \tag{20}$$

$$\sum_{n=1}^N \sum_{i=1}^I t_{ni}^k, \sum_{i=1}^I \sum_{j=1}^J t_{ij}^k > 0 \tag{21}$$

$$\sum_{n=1}^N U_n \geq \sum_{h=1}^H V_h \tag{22}$$

$$\sum_{h=1}^H V_h \geq \sum_{n=1}^N \sum_{i=1}^I q_{ni}^k \tag{23}$$

$$\sum_{h=1}^H V_h \geq \sum_{i=1}^I \sum_{j=1}^J q_{ij}^k \tag{24}$$

$$\sum_{n=1}^N \sum_{i=1}^I \sum_{j=1}^J q_{nij}^k > 0 \tag{25}$$

$$\sum_{n=1}^N \sum_{i=1}^I \sum_{j=1}^J n + i + j \leq p_o \tag{26}$$

$$\sum_{i=1}^I q_i - \sum_{n=1}^N \sum_{i=1}^I q_{ni} = 0 \tag{27}$$

$$\sum_{j=1}^J q_j - \sum_{i=1}^I \sum_{j=1}^J q_{ij} = 0 \tag{28}$$

$$\sum_{i=1}^I \sum_{j=1}^J d_{ji}^k > 0 \tag{29}$$

$$\sum_{i=1}^I \sum_{j=1}^J t_{ji}^k > 0 \tag{30}$$

$$\sum_{h=1}^H V_h \geq \sum_{i=1}^I \sum_{j=1}^J q_{ji}^k \tag{31}$$

$$\sum_{i=1}^I q_i - \sum_{i=1}^I \sum_{j=1}^J q_{ji} = 0 \tag{32}$$

$$\int_0^{d_{ji}} 0.5\lambda\mu^2 (s1 / s2)d(s) \leq Y \tag{14}$$

The constraints outlined in the equations are as follows. Equation 19 stipulates that the number of front-loading warehouse points should not exceed the total front-loading warehouse points H. Equations 20 and 29 indicate that transport distance has no negative constraints. Equations 21 and 30 specify that transportation time must be non-negative. Equation 22 states that the total capacity of a front-loading warehouse should not exceed that of large distribution centres or hubs. Equation 23 requires the total capacity of the front-loading warehouse to be at least equal to the sum of goods distributed from large distribution centres or hubs to the front-loading warehouse. Equation 24 imposes the condition that the total capacity of the front-loading warehouse must be greater than or equal to the total goods delivered from the front-loading warehouse to the next level of consumers. Equation 25 enforces a non-negative constraint on cargo volume throughout the logistics operation process. Equation 26 sets an upper limit on the total number of nodes in the logistics operation process. Equations 27 and 28 ensure that the amount of goods delivered to and from the front-loading warehouse matches the amount received, preventing cargo deviation. Equation 31 limits the amount of goods delivered to the front-loading warehouse in the reverse section to not exceed the warehouse’s capacity. Equation 32 requires that the amount of goods delivered to the front-loading warehouse in the reverse section matches the amount received, with no cargo deviation. Equation 14 establishes a budget constraint for the reverse segment.

## 4. ALGORITHM SIMULATION AND CASE ANALYSIS

Initially, it is crucial to perform an analysis and evaluate the performance of two different optimisation algorithms individually. Subsequently, these algorithms can be integrated to develop a novel hybrid optimisation algorithm customised for case simulation.

### 4.1 Algorithmic simulation analysis

#### Basic state-of-the-art and performance simulation of invasive weed optimisation algorithms

The invasive weed optimisation algorithm (IWO) was first introduced by Mehrabian and Lucas in 2006. This algorithm mimics the growth and reproductive processes of weeds in natural environments and is considered an evolutionary approach. To assess the effectiveness of the IWO algorithm, the Rastrigin function will be utilised as the test objective. The Rastrigin function is a common non-linear multi-peak function with numerous significant and minor values in the search region, making it challenging to identify the global minimum. It is commonly used to evaluate the performance of search algorithms. The mathematical expression of the Rastrigin function is Equation 33 as follows.

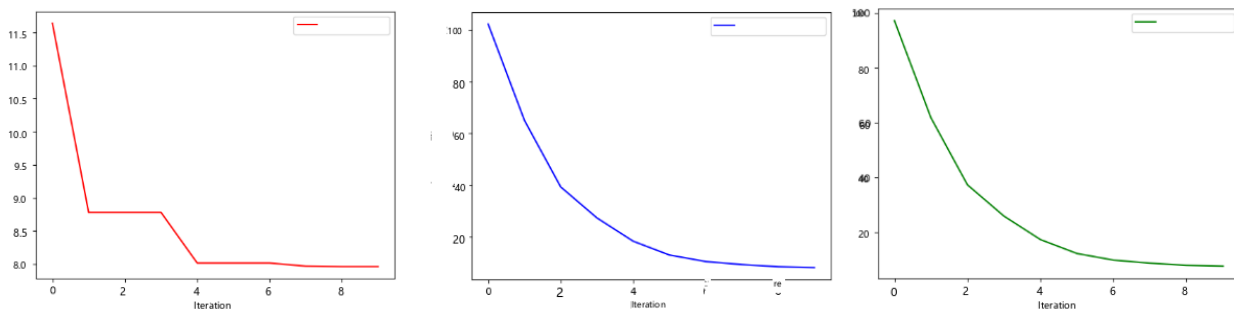
$$f(x_1, x_2) = 20 + x_1^2 + x_2^2 - 10\cos(2\pi x_1) - 10\cos(2\pi x_2) \tag{33}$$

The experimental conditions were defined by specific parameters, including an initial weed population size of 100, a maximum seed production of 5 per weed, an initial standard deviation of 0.1 and a final standard deviation of 0.01. The search was conducted within a two-dimensional range limited by the coordinates (-15, 15). The experiment entailed manipulating different numbers of iterations, namely 10, 30 and 50, each repeated 30 times to enable comparative analysis. The study results are elaborated in Table 1 and Figures 6-8. The comprehensive dataset is accessible for further scrutiny.

Table 1 – Comparison of data for different iterations

| The number of iterations          | 10                      | 30                        | 50                       |
|-----------------------------------|-------------------------|---------------------------|--------------------------|
| Optimal solution                  | [1.9913544, -1.9930144] | [-0.99438332, 1.98994947] | [0.99506742, 0.99463481] |
| Optimal fitness                   | 7.96198037627013        | 4.97485615269421          | 1.9899412538690378       |
| Average adaptation                | 30.179143470004288      | 12.346568045296241        | 5.670069026905775        |
| The average degree of convergence | 28.670186296504063      | 11.729239643031429        | 5.386565575560484        |

Note: The optimal average fitness is calculated from the fitness corresponding to the 15 optimal location points. According to the optimisation logic of the algorithm, like the optimal fitness, the smaller the value, the better. The same is below.

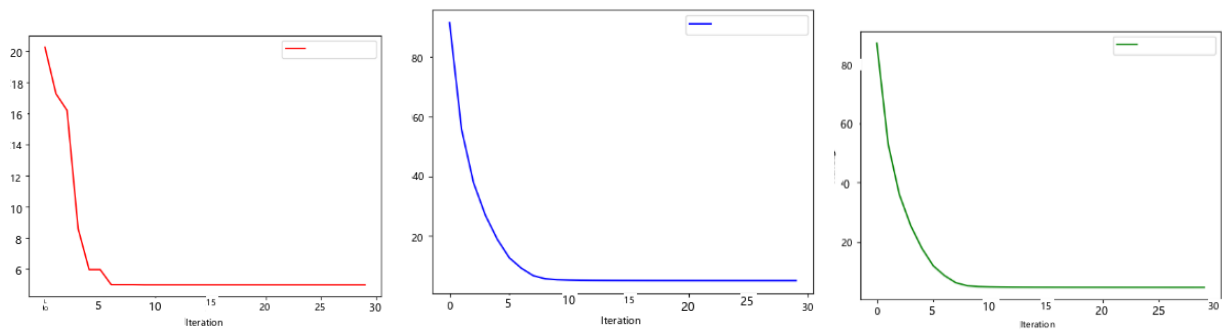


(1) Optimal fitness curve

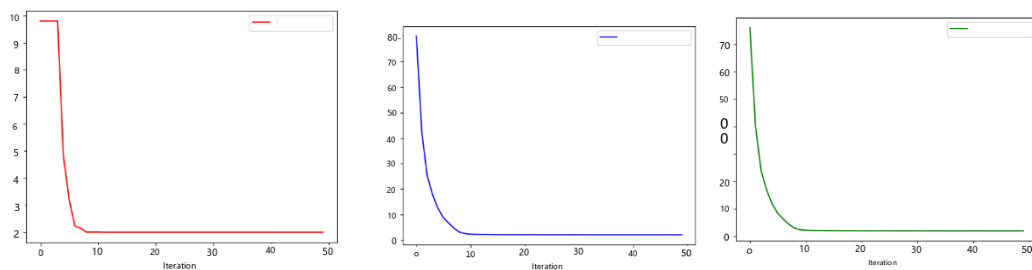
(2) Mean fitness curve

(3) Mean convergence curve

Figure 6 – Curves of related data for 10 iterations



(1) Optimal fitness curve (2) Mean fitness curve (3) Mean convergence curve  
 Figure 7 – Curves of related data for 30 iterations



(1) Optimal fitness curve (2) Mean fitness curve (3) Mean convergence curve  
 Figure 8 – Curves of related data for 50 iterations

*Basic state-of-the-art and performance simulation of artificial fish schooling algorithms*

The artificial fish schooling algorithm is intended to mimic the random behaviours observed in fish schools, such as feeding, gathering and chasing each other’s tails, to efficiently search for the best solution on a global scale. To assess the effectiveness of this algorithm, the Sphere function is utilised as a test case. The Sphere function is a real function typically defined in a multidimensional space that represents all points on a Sphere with a single global minimum and no local minima. In the realm of multidimensional optimisation problems, utilising a high-dimensional representation of the Sphere function is a useful method for evaluating how well an algorithm in addressing problems with numerous variables. This approach aids in evaluating the algorithm’s capability to effectively converge towards the global minimum while avoiding being stuck in local minima. The functional form of the Sphere function is Equation 34 as follows.

$$f(x) = \sum_{i=1}^n x_i^2, \quad x \in [-10, 10], i = 1, 2, \dots, n \tag{34}$$

The test parameters were specified as follows: an initial population of 100 fish individuals, a field of view of 0.8, an individual step size of 0.5, an individual search speed of 1.2 and a maximum of 25 attempts. The experiments were conducted over 10, 15 and 20 cycles, with each cycle being repeated 30 times to enable comparisons within the search range of (-5, 5). The detailed data results are presented in Table 2, accompanied by Figures 9-11.

Table 2 – Comparison of data for different iterations

| The number of iterations          | 10                        | 15                        | 20                        |
|-----------------------------------|---------------------------|---------------------------|---------------------------|
| Optimal solution                  | [-0.00162623, 0.02358999] | [-0.0090385, -0.00994732] | [0.00943934, -0.00677041] |
| Optimal fitness                   | 0.0005591321328560483     | 0.0001806437015170644     | 0.00013493954659336377    |
| Average adaptation                | 11.838012336986575        | 9.988611066714347         | 7.760909713143216         |
| The average degree of convergence | 11.239072623638457        | 9.386731027361359         | 7.212912710124215         |

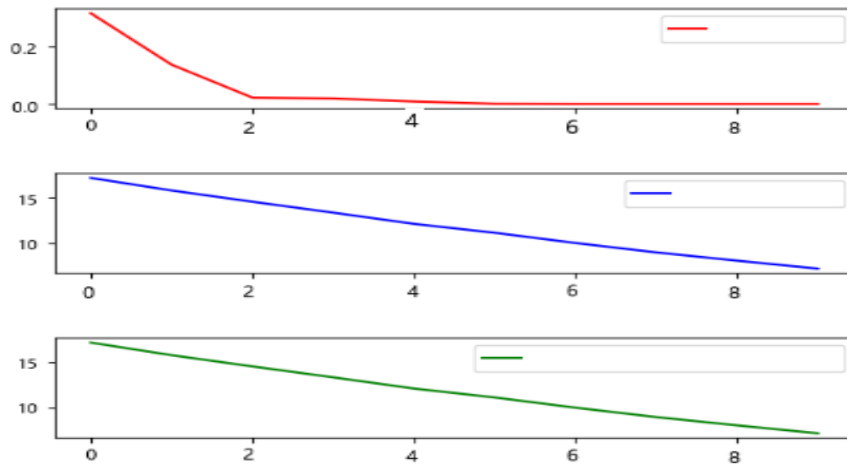


Figure 9 – 10 iterations

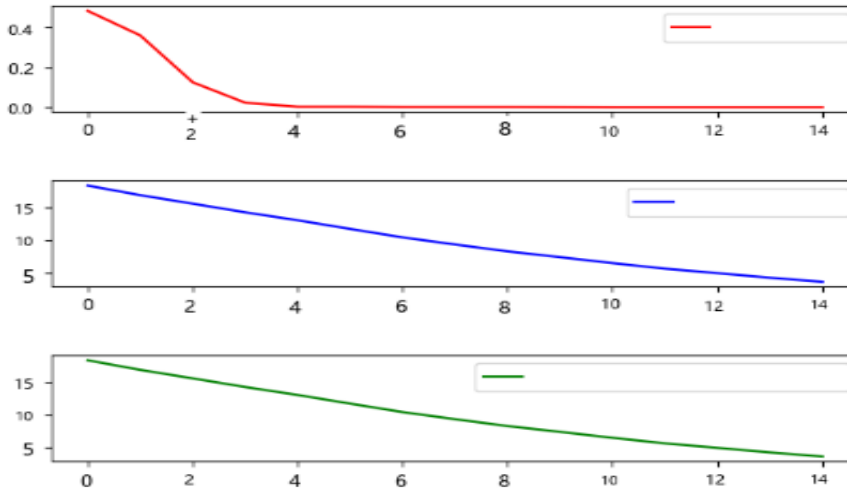


Figure 10 – 15 iterations

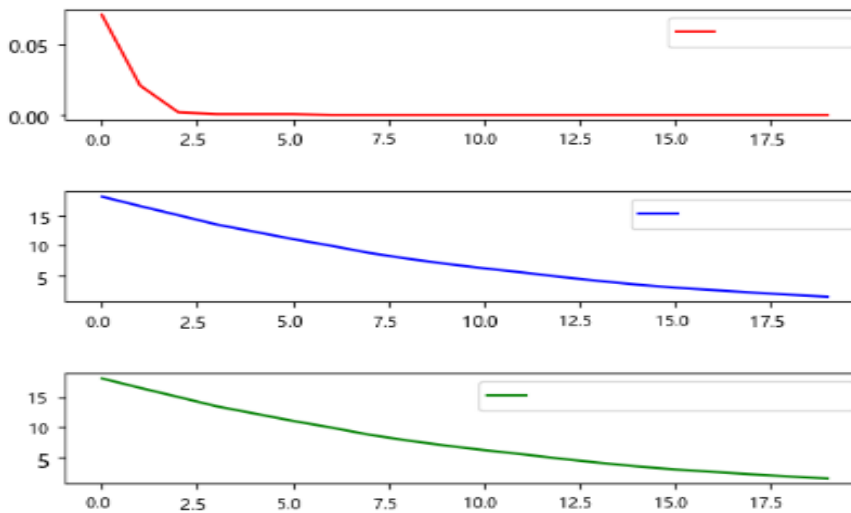


Figure 11 – 20 iterations

Note: The red line denotes the optimal adaptation, the blue line signifies the average adaptation and the green line indicates the average convergence. (The same applies below.)

The predominant concern related to the invasive weed optimisation algorithm revolves around the influence of different iteration durations on the algorithm’s efficacy. Examination of three separate datasets demonstrates a consistent trend: with an increase in the number of iterations, there is a gradual decrease in both the average fitness value and the average convergence value, leading to a more uniform pattern in the data. This phenomenon can be explained by the resemblance between the search path of the invasive weed optimisation algorithm and the optimisation curve. Consequently, the optimal fitness value gradually decreases, indicating a trend towards stability and consistency over time. The number of iterations plays a crucial role as a limiting factor affecting the convergence and optimal fitness of the optimisation process. Excessive iteration counts have the potential to impede individual agents from achieving optimal or enhanced solutions within the defined constraints, consequently jeopardising the quality of the solution. Moreover, inadequate configuration of additional algorithm parameters can worsen this problem. Furthermore, inefficiencies within the local search process, which may arise from suboptimal parameter configurations or algorithmic design, have the potential to cause repetitive searches, thereby substantially reducing the algorithm’s effectiveness and the accuracy of its outcomes.

*A description of the improved hybrid optimisation algorithm*

The main improvement focuses on adjusting the primary search algorithms to determine the existence of another person within a defined range. Upon identification, the individual undergoes a metamorphosis into a distinct entity. Additionally, the optimisation logic of the alternative algorithm has been enhanced to support the smooth advancement of the search process. The optimisation performance outcomes are elaborated below.

- Weed individuals. Once the parameters are initialised, the algorithm begins by searching for individuals classified as weeds based on the optimisation logic of the invasive weed optimisation algorithm. Following this, seeds are dispersed around the parent plant to create new individuals. The search mechanism of the artificial fish swarm algorithm is temporarily utilised to explore within a specific range of the parent to identify any artificial fish individuals. The judgment expression is outlined as follows are Equations 35-37:

$$R_y = \left(\frac{iter_{max} - iter}{iter_{max}}\right)^w \frac{X_v - X_i}{\|X_v - X_i\|} r \tag{35}$$

$$R_x = (X_v - X_i)r \tag{36}$$

$$d = \sqrt{(a_x - a_y)^2 + (b_x - b_y)^2} \tag{37}$$

where  $R_x$  and  $R_y$  represent the judgment radius of artificial fish and weed respectively, and  $d$  represents the straight-line distance between them. If  $d \leq R_x, R_y$ ,  $d \leq |R_x - R_y|$ , it means that there are artificial fish individuals within the search range indicating the need to transform the weed individuals into artificial fish individuals. Subsequently, the search process should proceed by utilising the optimisation principles of the artificial fish swarm algorithm. If no artificial fish are found within the search range, the optimisation logic of the invasive weed optimisation algorithm is employed to advance to the subsequent step. The objective of this stage is to eliminate search individuals with comparable distances, aiming to eliminate similar or duplicate solutions during the optimisation process and enhance the quality of solutions. During the amalgamation of new individuals with the existing ones from the parent generation, it is crucial to determine if the resultant sum exceeds the maximum capacity of the weed population. In such cases, when the total count surpasses the upper limit, the excess weed individuals will be transformed into artificial fish individuals. Subsequently, the algorithm will proceed with the search logic of the artificial fish population. The decision criterion is Equation 38 stated as follows:

$$N_{\#} = \left[ N_{\#} + \frac{(F_x - F_{min})}{(F_{max} - F_{min})} * (Seed_{max} - Seed_{min}) + Seed_{min} \right] - N_{\#} \tag{38}$$

where  $N_{\#}$  denotes the current number of parent weed individuals; the  $N_{\#}$  denotes the upper capacity limit of the weed individual; the  $N_{\#} \geq 0$ . If the number of individuals does not exceed the upper limit of the population capacity, then continue with the next step of the invasive weed optimisation algorithm. If the number of individuals stays below the upper limit of the population capacity, the next stage of the invasive weed optimisation algorithm continues with the exploration process. This stage is designed to reduce the number of individuals that may become stuck in the local search, thus reducing redundant searches and improving search efficiency.

- Artificial fish individuals. Following the execution of basic behaviours such as grouping, tail chasing and foraging, the artificial fish entities in the invasive weed optimisation algorithm utilise a search mechanism to locate weed individuals in proximity. This mechanism entails searching within a designated range of the

current artificial fish individuals to determine the existence of weed individuals. The decision-making process is outlined as follows in Equations 39-40.

$$R_x = \left(\frac{iter_{max} - iter}{iter_{max}}\right)^w (X_v - X_i)r \tag{39}$$

$$R_y = \left[\frac{(Fx - F_{min})}{(F_{max} - F_{min})}\right]^w \frac{X_v - X_i}{\|X_v - X_i\|} r \tag{40}$$

$$d = \sqrt{(a_x - a_y)^2 + (b_x - b_y)^2} \tag{37}$$

At this point, if  $d \leq R_x, R_y$ ,  $d \leq |R_x - R_y|$ , it means that there are weed individuals within the search range and necessitates the conversion of artificial fish individuals into weed individuals. Subsequently, the search process should persist following the optimisation principles of the invasive weed optimisation algorithm. If no weeds are present within the search range, the optimisation logic of the artificial fish swarm algorithm is employed to advance to the subsequent step. This step also aids in the elimination of solutions that are near each other, thereby preventing redundant searches for solutions and enhancing the quality of the solutions. The flow chart of the hybrid optimisation algorithm is shown in Figure 12.

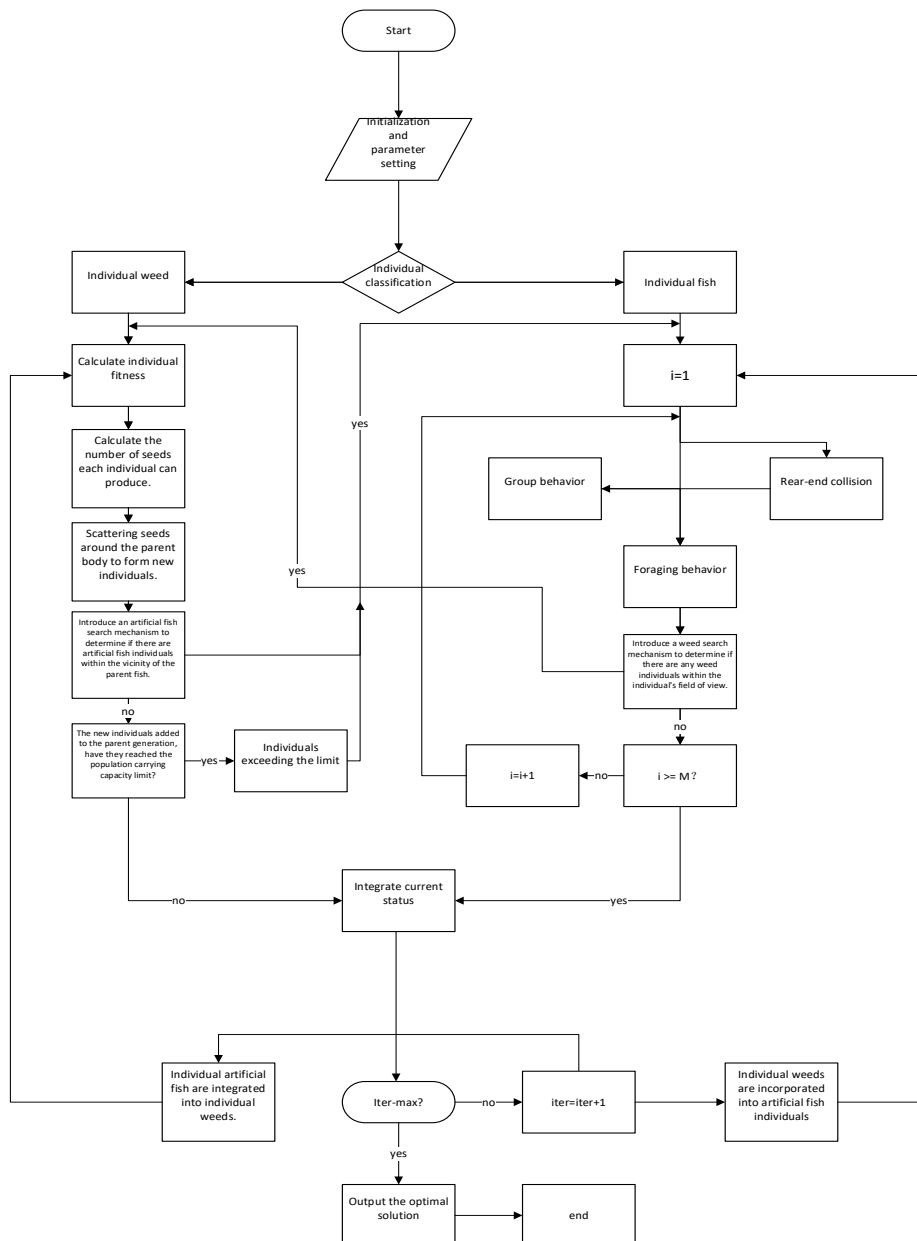


Figure 12 – Flow chart of weed-fish population mixed optimisation algorithm



The specific optimisation steps of the hybrid optimisation algorithm are as follows.

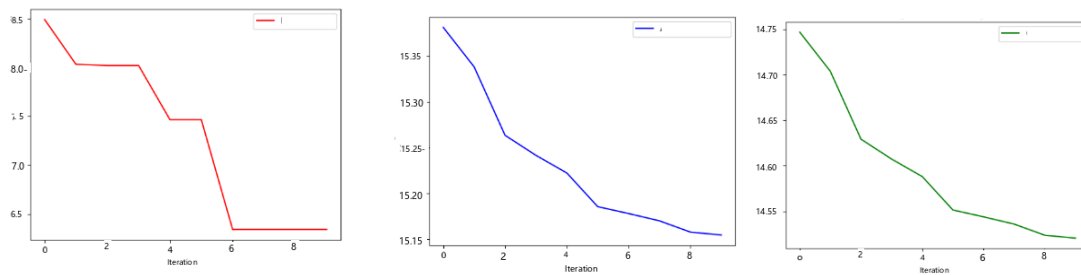
- Step 1. Set parameters, initialise parameters and classify individuals. Generate the initial weed population and the initial artificial fish population, and set the iteration times  $iter$  and the upper limit of the maximum iteration times  $iter_{max}$ , upper limit of total number of individuals  $N$ , number of weed individuals  $number_{grass}$ , number of artificial fish individuals  $number_{fish}$ , the upper limit of the number of seeds reproduced  $S_{max}$  and lower bounds  $S_{min}$ , nonlinear reconciliation factor  $w$ , individual movement step, visual field range  $visual$ , visual field floating range  $random\_visual$ , maximum number of attempts  $max\_try\_number$ , individual search speed  $step\_velocity$ .
- Step 2. Calculate the adaptation level of weed individuals and initialise the bulletin board  $M$ , which is utilised to document the condition of each artificial fish individual. The bulletin board documents the optimal state of the artificial fish during the optimisation process among other records.
- Step 3. The number of seeds produced by each weed individual and dispersed around their respective parents to establish new individuals was calculated. The artificial fish individuals opted to engage in flocking or tail chasing behaviours before uniformly carrying out foraging behaviours.
- Step 4. The algorithm involves searching for artificial fish individuals around the weed parent. If found, they are transformed into artificial fish individuals and the process returns to the artificial fish individuals' section in step 2. Similarly, the algorithm searches for weed individuals around the artificial fish. If found, they are transformed into weed individuals, and the process returns to the weed individuals' section in step 2. If the item is not found, the search should be continued.
- Step 5. The evaluation involves determining whether the combined population size of the new weed individual and the parent individual surpasses the upper limit of the population capacity. If the sum exceeds the limit, the surplus portion will be converted into an artificial fish individual and reintegrated into the artificial fish individual section of step 2. If the sum does not exceed the limit, the search process continues. Subsequently, a comparison is made between the status of the artificial fish individual post-behaviour completion and the status on the bulletin board. If the status is superior to that on the bulletin board, the status is updated to reflect the current state of the artificial fish, and the search continues. If the status is not better than that on the bulletin board, the status of individual  $i+1$  is updated, and the process returns to the artificial fish individual section of step 3. If the current state surpasses that of the bulletin board, the state of the individual  $i+1$  should be updated, and the process should return to step 3 for the individual artificial fish. Then unify the current algorithm progress status, determine whether the current iteration number  $iter$  reaches the maximum iteration number  $iter_{max}$ . If it is reached, go to step 7, on the contrary, go to step 6.
- Step 6. Iterate  $iter+1$ , return to step 2, convert the individual type, repeat the next round of search with another algorithm's optimisation logic.
- Step 7. Output the optimal solution and end the search.

## 4.2 Hybrid optimisation algorithm performance tests

The optimisation performance of the hybrid optimisation algorithm proposed for weed and fish schools was assessed by employing Rastrigin and Sphere functions as test cases. The evaluation included a comparison with the invasive weed optimisation algorithm and artificial fish school algorithm operating independently. The Rastrigin function was initially tested using specific parameters. These included 50 initial weed individuals, 50 initial artificial fish individuals, a total limit of 100 individuals, a maximum of 5 seeds per weed individual, an initial standard deviation of 0.1, a final standard deviation of 0.01, a field of view range of 0.8, an individual moving step of 0.5, an individual searching speed of 1.2, a maximum number of attempts set at 25, and the search was conducted within a 2-dimensional range of (-15,15). The experiment was conducted over 10, 30 and 50 iterations, with each iteration repeated 30 times for comparative analysis. The results are displayed in Table 3, Figure 13-15.

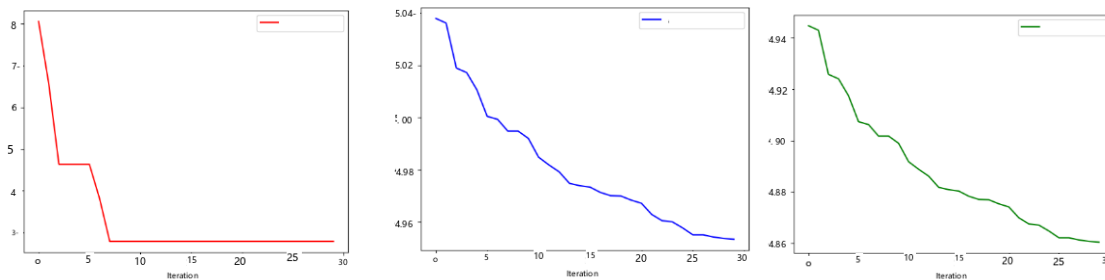
Table 3 – Comparison of data for different iterations

| The number of iterations          | 10                       | 30                       | 50                       |
|-----------------------------------|--------------------------|--------------------------|--------------------------|
| Optimal solution                  | [3.94397799, 0.02964038] | [1.83217405, 0.15442816] | [0.14360209, 2.12738353] |
| Optimal fitness                   | 6.341897725607886        | 2.7934089288041974       | 1.3837656747251526       |
| Average adaptation                | 15.154711138044794       | 4.953427351696173        | 2.373889843197118        |
| The average degree of convergence | 14.520521365484006       | 4.860313720736032        | 2.3462145297026153       |



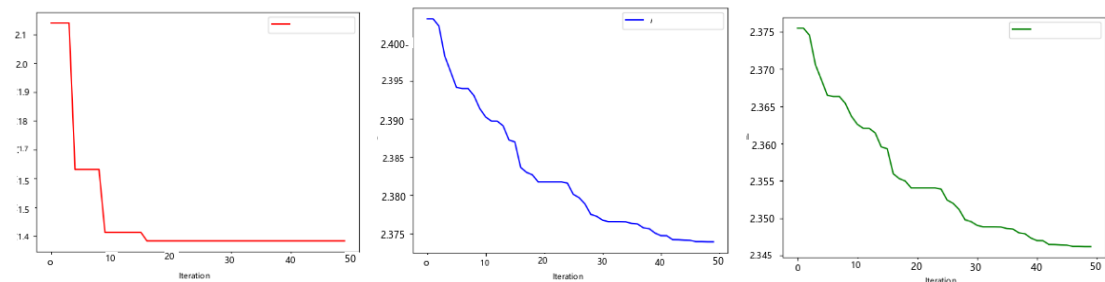
(1) Optimal fitness curve (2) Mean fitness curve (3) Mean convergence curve

Figure 13 – Curves of related data for 10 iterations



(1) Optimal fitness curve (2) Mean fitness curve (3) Mean convergence curve

Figure 14 – Curves of related data for 30 iterations



(1) Optimal fitness curve (2) Mean fitness curve (3) Mean convergence curve

Figure 15 – Curves of related data for 50 iterations

The Sphere function test was carried out using predefined parameters. The parameters comprised an initial population of 50 weed individuals and 50 artificial fish individuals, with a total population cap of 100. Each individual weed plant produced a maximum of five seeds, with the initial standard deviation set at 0.1, which decreased to 0.01 by the conclusion of the experiment. The field of view varied between 0.8, with a movement increment of 0.5, and a search velocity of 1.2 for each participant. The maximum number of attempts was limited to 25. The exploration was conducted in a two-dimensional space confined within the limits of (-5, 5) over 10, 15 and 20 iterations, with each iteration being repeated 30 times to facilitate comparative analysis. The outcomes of these examinations are delineated in Table 4, along with Figures 16-18.

Table 4 – Comparison of data for different iterations

| The number of iterations          | 10                        | 15                       | 20                       |
|-----------------------------------|---------------------------|--------------------------|--------------------------|
| Optimal solution                  | [0.20903342, -0.15899793] | [0.20408493, 0.09557857] | [0.22601263, 0.01071483] |
| Optimal fitness                   | 0.00027590125534443803    | 0.00013542911932418032   | 0.0001023930317012945    |
| Average adaptation                | 8.463768531431102         | 6.859010948125059        | 6.522436187656403        |
| The average degree of convergence | 8.431980087819916         | 6.831607301620439        | 6.481495015069088        |

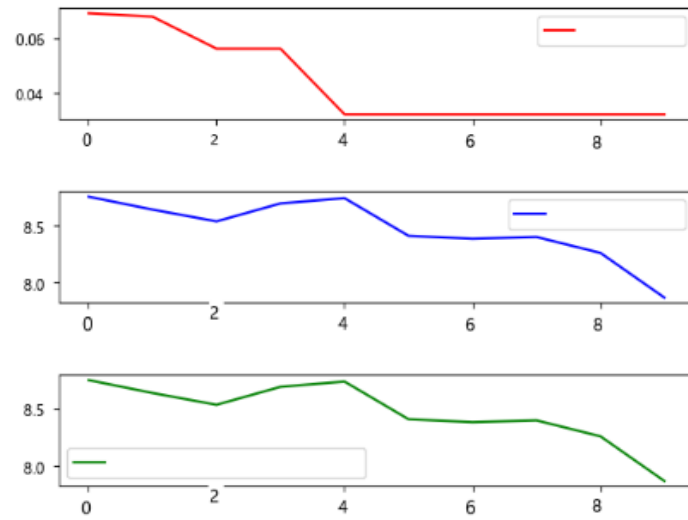


Figure 16 – 10 iterations

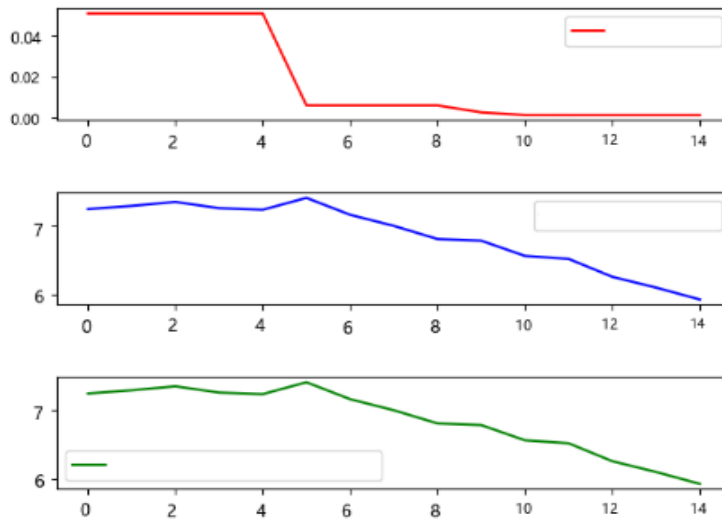


Figure 17 – 15 iterations

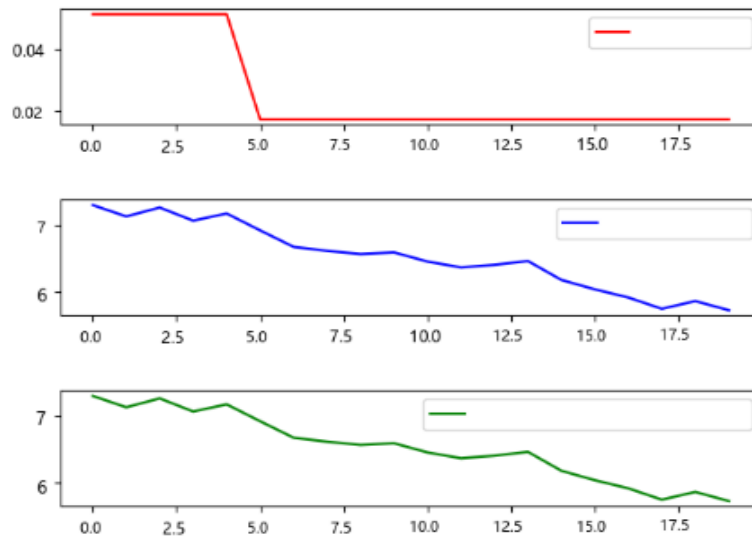


Figure 18 – 20 iterations

The ultimate outcomes achieved through the weed-fish hybrid optimisation algorithm are contrasted with the results obtained from two distinct algorithms, as illustrated in *Tables 5 and 6*.

*Table 5 – Comparison of data results with Rastrigin function*

| The number of iterations                | 10                       | 30                        | 50                       |
|---|--------------------------|---------------------------|--------------------------|
| Grass optimal solution                  | [1.9913544, -1.9930144]  | [-0.99438332, 1.98994947] | [0.99506742, 0.99463481] |
| Mixed optimal solution                  | [3.94397799, 0.02964038] | [1.83217405, 0.15442816]  | [0.14360209, 2.12738353] |
| Grass optimal fitness                   | 7.96198037627013         | 4.97485615269421          | 1.9899412538690378       |
| Mixed optimal fitness                   | 6.341897725607886        | 2.7934089288041974        | 1.3837656747251526       |
| Grass average adaptation                | 30.179143470004288       | 12.346568045296241        | 5.670069026905775        |
| Mixed average adaptation                | 15.154711138044794       | 4.953427351696173         | 2.373889843197118        |
| The grass average degree of convergence | 28.670186296504063       | 11.729239643031429        | 5.386565575560484        |
| The mixed average degree of convergence | 14.520521365484006       | 4.860313720736032         | 2.3462145297026153       |

*Table 6 – Comparison of data results with sphere function*

| The number of iterations                | 10                        | 15                        | 20                        |
|---|---------------------------|---------------------------|---------------------------|
| Fish optimal solution                   | [-0.00162623, 0.02358999] | [-0.0090385, -0.00994732] | [0.00943934, -0.00677041] |
| Mixed optimal solution                  | [0.20903342, -0.15899793] | [0.20408493, 0.09557857]  | [0.22601263, 0.01071483]  |
| Fish optimal fitness                    | 0.0005591321328560483     | 0.0001806437015170644     | 0.00013493954659336377    |
| Mixed optimal fitness                   | 0.00027590125534443803    | 0.00013542911932418032    | 0.0001023930317012945     |
| Fish average adaptation                 | 11.838012336986575        | 9.988611066714347         | 7.760909713143216         |
| Mixed average adaptation                | 8.463768531431102         | 6.859010948125059         | 6.522436187656403         |
| The fish average degree of convergence  | 11.239072623638457        | 9.386731027361359         | 7.212912710124215         |
| The mixed average degree of convergence | 8.431980087819916         | 6.831607301620439         | 6.481495015069088         |

Through the comparison of *Table 5* and *Table 6*, it is not difficult to find that the hybrid optimisation algorithm is almost omni-directional due to two independent algorithms. Taking the optimal fitness as an example, in the Rastrigin function test, the optimal fitness of the hybrid optimisation algorithm under 10, 30 and 50 iterations is 20.3%, 43.8% and 30.5% less than that of the independent weed algorithm, respectively. In the Sphere test function, the optimal fitness of the hybrid optimisation algorithm is 50.8%, 25% and 23.9% lower than that of the independent fish swarm algorithm. The comparative analysis shows that the hybrid optimisation algorithm, which combines weed fish swarm with other algorithms, outperforms individual algorithms across various metrics. This hybrid approach helps identify more suitable optimal fitness values and surpasses standalone algorithms in average fitness and convergence rates. As a result, there is a significant improvement in overall operational efficiency. The hybrid optimisation algorithm shows higher search activity in the initial phases compared to the independent algorithm. Even in the advanced stages of the search process, when search intensity decreases, the hybrid algorithm maintains a steady level of search activity. This characteristic helps prevent premature convergence, a common problem in independent algorithms where they tend to converge to local optima or keep exploring the same solutions. The study introduces a hybrid optimisation algorithm called the weed fish swarm algorithm, which effectively generates optimal results by avoiding local optima, maintaining strong search capabilities, and enhancing optimisation efficiency. Ultimately, the algorithm generates more precise and effective solutions.

### 4.3 Model simulation – a case study of Nanjing City

#### *Analysis of the problem of establishing a front-loading warehouse*

This chapter centres on the location issue concerning the establishment of a front-loading warehouse in Nanjing. The research entails the selection of 8 significant distribution centres or hubs located in the primary city of Nanjing (excluding Lishui and Gaochun districts) and 300 representatives from regional consumer terminals spread across

the city in 2023. The aim is to determine 50 optimal sites for strategically locating warehouses in the primary urban centre and its vicinity. *Table 7* presents relevant data for the selected distribution centres or hubs, while *Table 8* displays data for the front-loading warehouses under consideration, and *Table 9* provides information on the regional consumer terminals.

*Table 7 – Data on large distribution centres or hubs*

| Large distribution centres or hubs                       | Latitude and longitude | Average daily shipments/t |
|--|------------------------|---------------------------|
| Zhonecai Wholesale Market                                | (118.88, 31.98)        | 3,040                     |
| Tian Yin Shan Wholesale Market                           | (118.86, 31.94)        | 1,780                     |
| Maqun Logistics Centre                                   | (118.90, 32.07)        | 1,050                     |
| Jiangbei Agricultural and Side Products Wholesale Market | (118.78, 32.30)        | 2,200                     |
| Yuhua Logistics Centre                                   | (118.64, 31.92)        | 960                       |
| Runfeng Agricultural and Side Products Wholesale Market  | (118.80, 32.11)        | 800                       |
| Xingang Food Market                                      | (118.86, 32.14)        | 1,980                     |
| Jinling Logistics Jiangbei Distribution Centre           | (118.72, 32.20)        | 1,320                     |

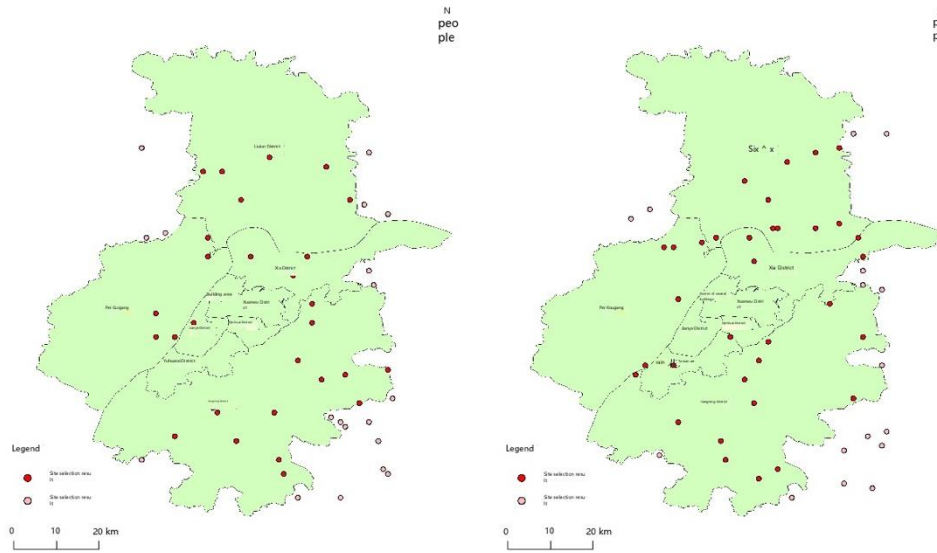
*Table 8 – Data related to the selected front-loading warehouse*

| The area in which the front-loading warehouse to be selected is located | Average daily total shipments/t | Estimated daily average recovery amount/t |
|---|---------------------------------|---|
| Qinhuai District  | 828                             | 198                                       |
| Gulou District  | 995                             | 203                                       |
| Xuanwu District   | 936                             | 176                                       |
| Jianye District   | 851                             | 142                                       |
| Yuhuatai District   | 2,003                           | 279                                       |
| Jiangning District  | 3,732                           | 501                                       |
| Qixia District  | 698                             | 168                                       |
| Pukou District  | 1,459                           | 180                                       |
| Liuhe District  | 1,628                           | 353                                       |

*Table 9 – Data related to end-consumer regional collections*

| End-consumer regional pools | Average daily receipt/t | Estimated daily average shipment/t |
|-----------------------------|-------------------------|------------------------------------|
| Qinhuai District            | 1,351                   | 226                                |
| Gulou District              | 1,842                   | 308                                |
| Xuanwu District             | 932                     | 156                                |
| Jianye District             | 913                     | 153                                |
| Yuhuatai District           | 786                     | 131                                |
| Jiangning District          | 2,539                   | 425                                |
| Qixia District              | 1,169                   | 196                                |
| Pukou District              | 1,683                   | 281                                |
| Liuhe District              | 1,915                   | 324                                |

Given the distinctive features of the administrative region and the demographic trends near Nanjing, this research has established a precise set of coordinates encompassing the target area and its adjacent regions, mirroring the central urban zone of Nanjing. This approach aims to optimise the pertinent calculations and processes involved in site selection. The algorithm model parameters consist of 50 individuals each for the weed and artificial fish populations, with a maximum capacity limit of 100. The model additionally stipulates a maximum of 30 iterations, an individual movement step size of 0.5, and an individual field of view range of 0.8. Following 30 iterations, distribution maps depicting the locations of pre-positioned warehouse sites under two distinct models are shown in Figure 19.



(1) Conventional model front-loading warehouse (2) Inverse model front-loading warehouse  
 Figure 19 – Distribution of front-loading warehouses

Within the dataset, the dark-coloured points represent the outcomes of site selection within the administrative boundaries of Nanjing, whereas the light-coloured points indicate the site selection outcomes outside this area. The site selection result diagram indicates that in the traditional model, the distribution of site selection points tends to follow the optimisation trajectory of the algorithm, emphasising the coverage rate of each region and resulting in more dispersed site selection points with a more evenly distributed actual distance between them. Conversely, the reverse model’s site selection is more focused and directional, with multiple points located in high-demand areas to meet customer needs, reflecting the function of front-loading warehouse in this model. Notably, Jiangning District, Liuhe District, Pukou District and Qixia District exhibit the largest and most extensive distribution of site selection points in the reverse model. This aligns with a 2023 report from the Nanjing Municipal Government indicating that these four districts account for nearly 47.2% of the total population in Nanjing’s main urban areas – a pattern consistent with population density as well as production and economic activities. Moreover, Table 10 presents the comprehensive average daily cost information for the two separate models:

Table 10 – Average daily total cost data

|                                       | The traditional front-loading warehouse model | The reverse front-loading warehouse model |
|---------------------------------------|---|---|
| Average daily total cost of model/RMB | 1,174,056.4                                   | 1,103,045.6                               |

Sensitivity analysis

A sensitivity analysis is performed to fully understand the influence of specific key parameters on total costs. The aim is to discover innovative approaches for cost control and to improve the efficiency of logistics networks. To optimise the model resolution process and improve data accuracy, it is necessary to adjust the default data in both models concurrently, whether by increasing or decreasing them.

- Unit transportation cost. By increasing the unit transportation cost by 10% and keeping the rest of the parameters unchanged, the total cost data obtained after solving are shown in *Table 11*.

*Table 11 – Analysis of unit transportation costs*

|                                       | <b>The traditional front-loading warehouse model</b> | <b>The reverse front-loading warehouse model</b> |
|---------------------------------------|--|--|
| Average daily total cost of model/RMB | 1,220,553.8  | 1,185,557.8                                      |

- Unit time cost. By increasing the unit time cost by 10% and keeping the rest of the parameter data unchanged, the total cost data obtained after solving are shown in *Table 12*.

*Table 12 – Analysis of unit time costs*

|                                       | <b>The traditional front-loading warehouse model</b> | <b>The reverse front-loading warehouse model</b> |
|---------------------------------------|--|--|
| Average daily total cost of model/RMB | 1,196,902.2  | 1,132,935.1                                      |

- Unit cost of goods loss. Increase the unit cost of goods loss by 10%, the rest of the parameter data remain unchanged, after solving the total cost of data as shown in *Table 13*.

*Table 13 – Analysis of unit damage costs*

|                                       | <b>The traditional front-loading warehouse model</b> | <b>The reverse front-loading warehouse model</b> |
|---------------------------------------|--|--|
| Average daily total cost of model/RMB | 1,187,144.4  | 1,121,766.1                                      |

- Fixed cost. By increasing the fixed cost by 10% and keeping the rest of the parameters unchanged, the total cost data obtained after solving are shown in *Table 14*.

*Table 14 – Analysis of fixed costs*

|                                       | <b>The traditional front-loading warehouse model</b> | <b>The reverse front-loading warehouse model</b> |
|---------------------------------------|--|--|
| Average daily total cost of model/RMB | 1,207,610.8  | 1,149,572.3                                      |

The analysis results indicate that a 10% increase in the unit transportation cost, unit time cost, unit cargo damage cost and fixed cost results in a corresponding rise in total costs of 4% and 7.5% for the traditional and reverse models, 1.9% and 2.7%, 1.1% and 1.7%, 2.9% and 4.2%, respectively.

## 5. CONCLUSION AND FUTURE OUTLOOK

The updated configuration of the reverse front-loading warehouse network model typically leads to a 6.4% decrease in overall expenses in contrast to the traditional front-loading warehouse model. The reduction in costs can be attributed to the economic advantages obtained from the customer utility of the reverse section, which assists in mitigating specific expenses. Moreover, the repositioning of front-loading warehouse in the reverse front-loading configuration plays a significant role in reducing the total expenses associated with the network model. The sensitivity analysis revealed that alterations in parameters result in diverse effects on overall costs, which can be classified into three distinct levels. The unit transportation cost has the most substantial impact on total costs among these factors. For example, a 10% rise in transportation expenses results in around a 4% increase in costs for the traditional model and a 7.5% increase for the reverse model. Hence, transportation expenses should be considered a crucial factor to monitor. While the costs associated with unit time and cargo damage may have a relatively smaller influence on overall expenses, they should not be overlooked, particularly in certain situations. Furthermore, based on the site selection results, the front-loading warehouse in the reverse model emphasises prioritising high-demand coverage by establishing

multiple site selection points in areas with high demand. This necessitates a focused approach to these high-demand areas during planning.

In densely populated urban areas such as Nanjing, the establishment of supplementary front-loading warehouses is essential to meet consumer demands, given the expansive urban sprawl and significant population size. This study presents theoretical concepts for developing a reverse front-loading position network model. It highlights the importance of considering practical implementation factors, including market dynamics, demand distribution, population density and policy frameworks. When choosing sites for front-loading warehouses, it is essential to conduct a comprehensive assessment of cost considerations and specific circumstances to meet goals such as minimising losses of perishable agricultural products, reducing logistics costs and improving customer satisfaction.

## ACKNOWLEDGEMENTS

This article is supported by the Talent Introduction Project (NY219168) of Nanjing University of Posts and Telecommunications and the Natural Science Foundation Incubation Project (NY220214) of Nanjing University of Posts and Telecommunications. I would like to express my sincere gratitude for this.

## REFERENCES

- [1] Almeida P, Crispiniano Garcia R, Pallavicini Fonseca A. advances in modelling of the integrated production logistics in sugarcane harvest. *Promet-Traffic & Transportation*. 2022;34(4):595–608. DOI: 10.7307/ptt.v34i4.4012.
- [2] Ge H, et al. Research on emergency logistics model of agricultural products based on coupling of petri net and blockchain. *Promet-Traffic & Transportation*. 2021;33(6):883–891. DOI: 10.7307/ptt.v33i6.3845.
- [3] Jiang Y, Bian B, Zheng B, Chu J. A time space network optimization model for integrated fresh fruit harvest and distribution considering maturity. *Computers & Industrial Engineering*. 2024;110029. DOI: 10.1016/j.cie.2024.110029.
- [4] Ulloa R, Villalobos, JR. Impact of special-denomination label constraints on fresh produce supply chains. *Computers & Industrial Engineering*. 2022;173:108742. DOI: 10.1016/j.cie.2022.108742.
- [5] Chen J, Liao W, Yu C. Route optimization for cold chain logistics of front warehouses based on traffic congestion and carbon emission. *Computers & Industrial Engineering*. 2021;161:107663. DOI: 10.1016/j.cie.2021.107663.
- [6] Guan X, Li G. Optimization of cold chain logistics vehicle transportation and distribution model based on improved ant colony algorithm. *Procedia Computer Science*. 2023;228:974–982. DOI: 10.1016/j.procs.2023.11.128.
- [7] Gong C, et al. Logistics sourcing of e-commerce firms considering promised delivery time and environmental sustainability. *European Journal of Operational Research*. 2024;317(1):60–75. DOI: 10.1016/j.ejor.2024.02.026.
- [8] Rahmanifar G, et al. Integrated location and routing for cold chain logistics networks with heterogeneous customer demand. *Journal of Industrial Information Integration*. 2024;38:100573. DOI: 10.1016/j.jii.2024.100573.
- [9] Li D, Li K. A multi-objective model for cold chain logistics considering customer satisfaction. *Alexandria Engineering Journal*. 2023;67:513–523. DOI: 10.1016/j.aej.2022.12.067.
- [10] Garai A, Sarkar B. Economically independent reverse logistics of customer-centric closed-loop supply chain for herbal medicines and biofuel. *Journal of Cleaner Production*. 2022;334:129977. DOI: 10.1016/j.jclepro.2021.129977.
- [11] Chen Q, Liu Z, Tian L, Qin X. In-store, pre-warehouse, or store-and-warehouse integration: Strategic analysis for neighborhood fresh product retail modes. *Computers & Industrial Engineering*. 2023;177:109085. DOI: 10.1016/j.cie.2023.109085.
- [12] Jiang H, Wu T, Ren X, Gou L. Optimisation of multi-type logistics uav scheduling under high demand. *Promet-Traffic & Transportation*. 2024;36(1):115–131. DOI: 10.7307/ptt.v36i1.261.
- [13] Govindan K, Gholizadeh H. Robust network design for sustainable-resilient reverse logistics network using big data: A case study of end-of-life vehicles. *Transportation Research Part E: Logistics and Transportation Review*. 2021;149:102279. DOI: 10.1016/j.tre.2021.102279.
- [14] Labelle A, Frayret JM. First-mile reverse logistics: An agent-based modelling and simulation application for glass bottle recovery. *Journal of Cleaner Production*. 2023;422:138574. DOI: 10.1016/j.jclepro.2023.138574.



- [15] Ermes T, Niemann W. Managing omni-channel reverse logistics risk during supply chain disruption recovery in the South African fashion industry. *Journal of Transport and Supply Chain Management*. 2023;17:932. DOI: 10.4102/jtscm.v17i0.932.
- [16] Ahmadi S, Shokouhyar S, Amerioun M, Tabrizi NS. A social media analytics-based approach to customer-centric reverse logistics management of electronic devices: A case study on notebooks. *Journal of Retailing and Consumer Services*. 2024;76:103540. DOI: 10.1016/j.jretconser.2023.103540.
- [17] Bajgani SE, Saberi S, Toyasaki F. Designing a reverse supply chain network with quality control for returned products: Strategies to mitigate free-riding effect and ensure compliance with technology licensing requirements. *Technological Forecasting and Social Change*. 2023;195:122744. DOI: 10.1016/j.techfore.2023.122744.
- [18] Guo Y, Shahraki AA. Selection of rail station locations on an intercity route regarding maximum users' economic profits. *Promet-Traffic & Transportation*. 2023;35(4):595–606. DOI: 10.7307/ptt.v35i4.241.
- [19] Qichen O, Mi G, Meitong A, Yichen W. Road-rail intermodal hubs site selection based on road freight demand mining – A case from Beijing-Tianjin-Hebei region. *Promet-Traffic & Transportation*. 2024;36(3):492–507. DOI: 10.7307/ptt.v36i3.462.
- [20] Zhongyi J, et al. A risk-averse distributionally robust optimisation approach for drone-supported relief facility location problem. *Transportation Research Part E: Logistics and Transportation Review*. 2024;186:103538. DOI: 10.1016/j.tre.2024.103538.
- [21] Song J, Li B, Szeto WY, Zhan X. A station location design problem in a bike-sharing system with both conventional and electric shared bikes considering bike users' roaming delay costs. *Transportation research part E: logistics and transportation review*. 2024;181:103350. DOI: 10.1016/j.tre.2023.103350.
- [22] Kitthamkesorn S, Chen A, Ryu S, Opananon S. Maximum capture problem based on paired combinatorial weibit model to determine park-and-ride facility locations. *Transportation Research Part B: Methodological*. 2024;179:102855. DOI: 10.1016/j.trb.2023.102855.
- [23] Abdulvahitoğlu A, Vural D, Abdulvahitoğlu A. Optimising traffic safety–locating traffic gendarmes based on multi-criteria decision making. *Promet-Traffic & Transportation*. 2023;35(6):800–813. DOI: 10.7307/ptt.v35i6.318.
- [24] Liu C, Hou P. Dynamic modelling of cold chain logistics services under budget constraints for the delivery of fresh products in an urban area. *Applied Mathematical Modelling*. 2024;125:809-835. DOI: 10.1016/j.apm.2023.09.019.

## 基于生鲜农产品逆向物流的前置仓选址研究

习嘉睿，耿娜娜

### 摘要

前置仓的建设有助于在“最后一公里”处有效提高生鲜农产品的配送效率和质量。然而据数据表明，因需求预测失真等因素造成的生鲜农产品货损率逐年增长，主要表现在消费者无法第一时间按计划消耗掉原本所需的量，以及一些商家的真实需求量远高于需求预测量，这就导致相当数量的生鲜农产品无法按需消耗而浪费。基于此，本文研究并探讨了以前置仓为基础的生鲜农产品逆向物流模型的可行性，建立了以总成本最小化为目标的逆向模型，并对此类前置仓进行新的选址以满足逆生鲜农产品逆向物流的需求。在研究过程中通过运用改进的混合启发式优化算法寻觅最优结果，从而尽可能的减少生鲜农产品货损率，降低物流成本，有助于达到区域内的供需平衡。

### 关键词

物流选址；启发式算法；前置仓；逆向物流；生鲜农产品